

# Effect of Stress on Defect Transformation in $B^+$ and $Ag^+$ Implanted $HgCdTe/CdZnTe$ Structures

R.K. SAVKINA<sup>a</sup>, A.B. SMIRNOV<sup>a</sup>, A.I. GUDYMENKO<sup>a</sup>, V.P. KLADKO<sup>a</sup>, F.F. SIZOV<sup>a</sup>  
AND C. FRIGERI<sup>b</sup>

<sup>a</sup>V. Lashkaryov Institute of Semiconductor Physics at NASU, Prospect Nauki 41, 03028 Kiev, Ukraine

<sup>b</sup>CNR-IMEM Institute, Parco Area Delle Scienze, 37/A Fontanini, 43010 Parma, Italy

The results of X-ray, scanning electron microscopy and atomic force microscopy studies of near-surface regions of (111)  $Hg_{1-x}Cd_xTe$  ( $x = 0.223$ ) structures are presented. These structures were obtained by low-energy implantation with boron and silver ions. TRIM calculation of the depth dependences of impurity concentration and implantation-induced mechanical stresses in the layer near-surface regions has revealed that the low-energy implantation of  $HgCdTe$  solid solution with elements of different ionic radiuses ( $B^+$  and  $Ag^+$ ) leads to the formation of layers with significant difference in thickness (400 nm and 100 nm, respectively), as well as with maximum mechanical stresses differing by two orders of magnitude ( $1.4 \times 10^3$  Pa and  $2.2 \times 10^5$  Pa, respectively). The structural properties of the  $Hg_{1-x}Cd_xTe$  epilayers were investigated using X-ray high-resolution reciprocal space mapping.

DOI: [10.12693/APhysPolA.125.1003](https://doi.org/10.12693/APhysPolA.125.1003)

PACS: 61.72.uj, 81.16.Rf

## 1. Introduction

Ion implantation of  $HgCdTe$  (MCT) is a commonly used method for fabricating IR sensitive photovoltaic devices [1]. An implant, getting into the epitaxial layer, initiates an active restructuring of the defect structure of MCT, which changes the epilayer carrier type. This is facilitated by a low energy threshold for the intrinsic defect formation in MCT. As a result,  $n$ -on- $p$  (boron-implanted) [2] and  $p$ -on- $n$  (arsenic-implanted) [3] photodiodes are fabricated. At the same time, it is well known that ion implantation induces mechanical stress in MCT layers, which is a matter of paramount importance for solid-state devices, and has been exploited to improve their electrical and optical properties. It was shown that implantation-induced stress is an important factor influencing the depth of  $p$ - $n$  junctions in MCT-based structures [4]. Moreover, the existence of the built-in electric field in the strained MCT-based heterostructure results in the spatial separation of the nonequilibrium carriers and in the possibility of room temperature detection of the IR radiation [5].

This work aims at studying the influence of low-energy irradiation with  $B^+$  and  $Ag^+$  ions, as well as implantation-induced mechanical stresses, on the defect transformation in hetero-epitaxial  $Hg_{1-x}Cd_xTe/Cd_{1-y}Zn_yTe$  ( $x = 0.223$ ,  $y = 0.04$ ) structures.

## 2. Experimental

We have carried out a systematic study of mercury cadmium telluride thin films subjected to the low-energy ion implantation.  $p$ -type  $Hg_{0.777}Cd_{0.223}Te$  epilayers were grown on [111]-oriented semi-insulating  $Cd_{0.96}Zn_{0.04}Te$  substrates from a Te-rich solution at 450°C by liquid-phase epitaxy. The MCT layers to study were sorted into two groups — irradiated with  $B^+$  or  $Ag^+$  ions. Ion energy was about 100 keV and ion dose was about  $3 \times 10^{13} \text{ cm}^{-2}$ .

Post-implantation thermal treatments were carried out under an Ar atmosphere at 75°C for 5 h.

The structural characterization of the MCT samples was performed by X-ray diffraction (XRD) using a Panalytical Xpert-pro triple-axis X-ray diffractometer. X-rays were generated from copper linear fine-focus X-ray tube. The  $Cu K_{\alpha_1}$  line with a wavelength of 0.15418 nm was selected using a four-bounce (440) Ge monochromator. The experimental schemes allowed two cross-sections of reciprocal lattice sites to be obtained: normal ( $\omega$ -scanning) and parallel ( $\omega/2\theta$ -scanning) to the diffraction vector. The structural properties of the MCT epilayers were investigated using X-ray high-resolution reciprocal space mapping (HR-RSM). Grazing-incidence (GI) geometry was used for investigation of the near-surface region of the layers. The GI diffractograms have been collected by irradiating the samples at an incident angle ( $\theta_{inc}$ ) of 1°. The penetration depth at this incidence angle was  $\approx 400$  nm.

Contactless atomic force microscopy (AFM) with a NanoScope-IIIa Digital Instruments device and scanning electron microscopy (SEM) with a Tescan Mira3 LMU instrument were used for analysis of the surface morphology of the  $Hg_{1-x}Cd_xTe$ -based structures.

## 3. Results and discussion

It was found that the ion irradiation of the investigated samples gives rise to the formation of a remarkable variety of nanoscale patterns. SEM image of a periodic height modulations or “ripples” induced on the (111)  $Hg_{1-x}Cd_xTe$  surface by 100 eV  $B^+$  ions implantation are shown in Fig. 1a. Arrays of nanoscale mounds depicted in Fig. 1b is generated on the (111)  $Hg_{1-x}Cd_xTe$  surface as a result of 100 eV  $Ag^+$  ions implantation.

AFM characterization has revealed that the initial, before implantation, surface exhibits a grid of quasipores with average diameter  $\approx 100$  nm and the presence of

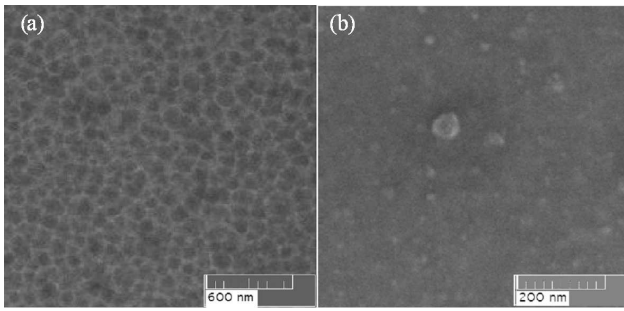


Fig. 1. SEM images of boron ions implanted (a) and silver ions implanted (b) (111)  $\text{Hg}_{1-x}\text{Cd}_x\text{Te}$  surface.

closely packed grains ranging from 40 to 80 nm in dimensions (see Fig. 2a). The root-mean-square roughness for a  $1 \times 1 \mu\text{m}^2$  surface area was around 3 nm. For samples implanted with boron ions the ordered grid of quasi-pores was not observed and the surface became denser (see Fig. 2b). The study of the microhardness with the use of a Shimadzu HMV-2000 device showed an increase of its value to 12%. The implantation with silver ions causes the emergence of a uniform array of nanoislands 5 to 25 nm in height and with a base diameter of 13 to 35 nm (Fig. 2c). Accordingly, the root-mean-square roughness increased.

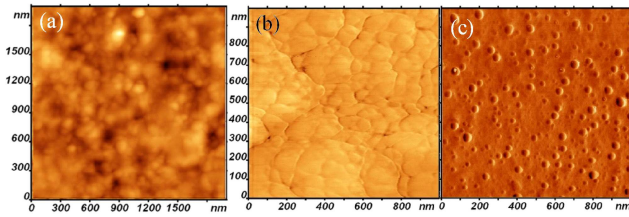


Fig. 2. AFM images of initial (a), boron implanted (b), and silver implanted (c) (111)  $\text{Hg}_{1-x}\text{Cd}_x\text{Te}$  surface.

Thereupon, X-ray rocking curves (RC) for MCT-based structures before and after implantation were obtained from the symmetrical  $\omega/2\theta$ -scanning. As seen in Fig. 3a, b, the RCs for boron implanted samples have symmetric form whereas the RCs for silver implanted samples have an asymmetric form and are characterized by a substantial shoulder on the high angle side. XRD results in the coherent-scattering region point out to the compression of the boron implanted MCT and tension of the silver implanted MCT layers.

Implantation with boron results in insignificant changes in the reciprocal space maps (RSMs). At the same time, two-dimensional RSMs of the intensity distribution around (111) sites for the MCT layer implanted with silver ions are depicted in Fig. 3c, d. It should be noted that a broadening of the diffraction pattern in the  $Q_x$  direction of silver implanted sample can indicate the formation of misoriented substructures produced by the implant. The investigation in the GI configuration was

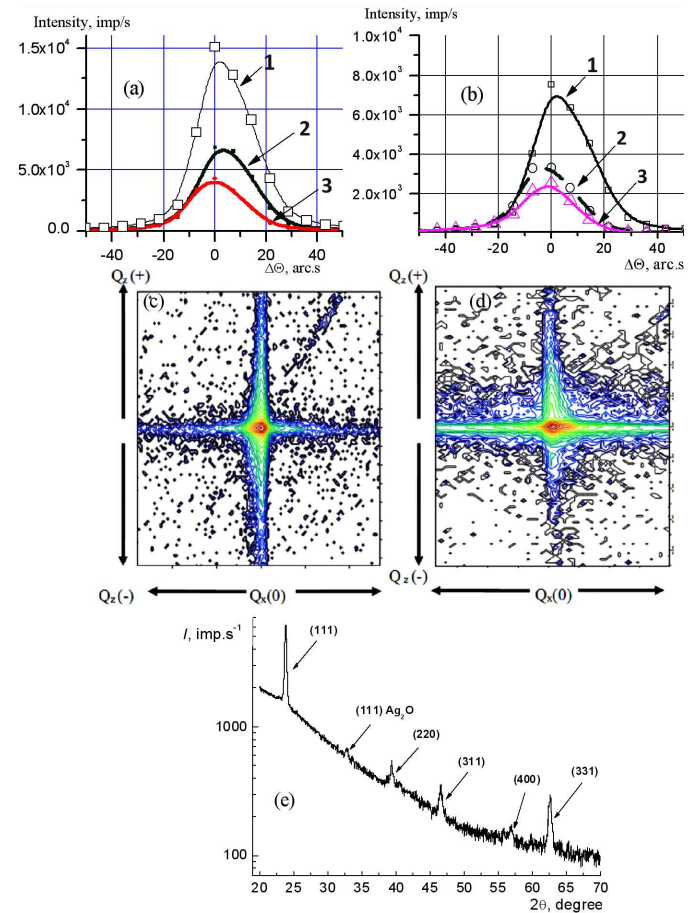


Fig. 3. HRXRD results. (a) X-ray rocking curves for typical  $\text{Hg}_{1-x}\text{Cd}_x\text{Te}$ -based structure: 1 — initial, 2 — boron implanted, 3 — annealed; (b) X-ray rocking curves for typical  $\text{Hg}_{1-x}\text{Cd}_x\text{Te}$ -based structure: 1 — initial, 2 — silver implanted, 3 — annealed; (c) HR-RSM for typical initial  $\text{Hg}_{1-x}\text{Cd}_x\text{Te}$ -based structure; (d) HR-RSM for silver implanted  $\text{Hg}_{1-x}\text{Cd}_x\text{Te}$ -based structure; (e) GI-XRD pattern ( $\theta_{\text{inc}} = 1^\circ$ ) for silver implanted  $\text{Hg}_{1-x}\text{Cd}_x\text{Te}$ -based structure.

also confirmed the formation of the polycrystalline phase in the near-surface region of the  $\text{HgCdTe}$  (ICDD PDF 00-051-1122) after silver implantation (see Fig. 3e). Besides, a new phase ( $\text{Ag}_2\text{O}$ , ICDD PDF 00-041-1104) was found.

Thus, the study of the surface morphology as well as the structural properties of  $\text{Hg}_{1-x}\text{Cd}_x\text{Te}$ -based structures before and after low-energy implantation indicates essential differences between  $\text{B}^+$  and  $\text{Ag}^+$  ion implantation.

The implantation of semiconductor systems is known to be accompanied by the insertion of a considerable number of defects as well as strain in the crystal lattice in the near-surface region. The mathematical simulation of the process of ion implantation with the use of the software package TRIM\_2008 allowed the parameters of the radiation-induced disordering region to be

determined. It was obtained that the energy transmitted by an implanted ion to the nuclear subsystem of the target by means of elastic interactions amounts to 79.2 eV/Å for B<sup>+</sup> ions and 27.68 eV/Å for Ag<sup>+</sup> ions. As we know, the enthalpy of Hg–Te bond formation is about 0.33 eV and for the Cd–Te bond  $\approx$  1.044 eV [6]. Therefore, we may assert that the track of a single ion forms a region around it in the HgCdTe target, where the crystal structure of the semiconductor is considerably damaged. The near-surface region of the target becomes saturated with point defects. In particular, in the HgCdTe system there are vacancies and mercury interstitial sites [7].

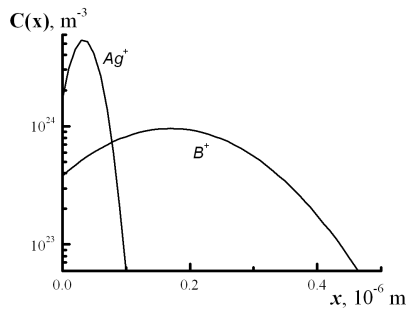


Fig. 4. Profiles of the Ag<sup>+</sup> and B<sup>+</sup> implant distributions in Hg<sub>1-x</sub>Cd<sub>x</sub>Te/Cd<sub>1-y</sub>Zn<sub>y</sub>Te structures.

The boundary of the HgCdTe crystal lattice distortion is determined by the implant distribution profile  $C(x)$  depicted in Fig. 4. The impurities are mainly located in the near-surface region of the Hg<sub>1-x</sub>Cd<sub>x</sub>Te layer 0.4/0.1  $\mu$ m in thickness. The thickness of a damaged layer determined from the results of ellipsometric measurements (of about 0.38/0.1  $\mu$ m, obtained in a previous work [8]) is close to the thickness of the layer in which the maximum implant concentration is observed.

The magnitude of the mechanical stresses created in the HgCdTe layer after implantation can be determined from the relation [9]:

$$\sigma(x) = \frac{C(x)\beta E}{1 - \nu},$$

where  $\nu$  is Poisson's ratio,  $E$  is the Young modulus,  $x$  is the coordinate, and  $C(x)$  is the distribution profile of an impurity introduced into the target. The coefficient of HgCdTe crystal lattice contraction introduced by the implant,  $\beta$ , was determined using the results of X-ray diffraction studies on the samples investigated [8]. The mechanical stresses that arise in the near-surface layer of an epitaxial MCT layer attain the maximum value of  $1.4 \times 10^3$  Pa for boron and  $2.2 \times 10^5$  Pa for silver implanted structure.

In our opinion, the distinction between the effects arising in the near-surface layer of an epitaxial MCT film owing to its treatment with boron or silver ions is associated with the opposite character of the deformations induced by inserting those ions into the crystal lattice. As was

shown in [4], implantation with ions of small radius (such as B<sup>+</sup>, with a radius of 1.17 Å [9]) stimulates the compression of the damaged layer, whereas the implantation with ions of radius comparable with that of Hg (in our case, these are Ag ions with a radius of 1.75 Å [9]) gives rise to tensile stress in the damaged layer, as confirmed by the XRD results obtained in this work.

#### 4. Conclusions

The influence of low-energy irradiation and implantation-induced mechanical stresses on the defect transformation in heteroepitaxial Hg<sub>1-x</sub>Cd<sub>x</sub>Te/Cd<sub>1-y</sub>Zn<sub>y</sub>Te ( $x = 0.223$ ,  $y = 0.04$ ) structures was investigated. Low-energy implantation of HgCdTe solid solution with B<sup>+</sup> and Ag<sup>+</sup>, elements of different ionic radiuses, leads to the formation of layers with significant difference in thickness (400 nm and 100 nm, respectively), as well as with maximum mechanical stresses that differ by two orders of magnitude from each other.

XRD results in the coherent-scattering region point to the compression of the boron implanted HgCdTe layers and tension of the silver implanted ones. AFM and SEM show the nanoscale surface structuring after implantation with Ag<sup>+</sup>. The extension of the near-surface region of the silver implanted HgCdTe and, accordingly, the contraction of the deeper layers may be the origin of the diffusion out of the silver ions to the surface and of the formation of metal oxide/semiconductor structures.

#### References

- [1] A. Rogalski, *Infrared Detectors*, 2nd ed., CRC Press, Boca Raton (FL) 2011.
- [2] S. Holander-Gleixner, B.L. Williams, H.G. Robinson, C.R. Helms, *J. Electron. Mater.* **26**, 629 (1997).
- [3] L. Mollard, G. Destefanis, N. Baier, J. Rothman, P. Ballet, J.P. Zanatta, M. Tchagaspanian, A.M. Papon, G. Bourgeois, J.P. Barnes, C. Pautet, P. Fougères, *J. Electron. Mater.* **38**, 1805 (2009).
- [4] H. Ebe, M. Tanaka, Y. Miyamoto, *J. Electron. Mater.* **28**, 854 (1999).
- [5] T. Kryshtab, R. Savkina, F. Sizov, A. Smirnov, M. Kladkevich, V. Samoylov, *Phys. Status Solidi C* **9**, 1793 (2012).
- [6] V.B. Lazarev, *Physical and Chemical Properties of Semiconductor Substances*, Nauka, Moscow 1979 (in Russian).
- [7] *Mercury Cadmium Telluride: Growth, Properties and Applications*, Eds. P. Capper, J.W. Garland, Wiley, Ltd, London 2011.
- [8] A. Smirnov, O. Lytvyn, V. Morozhenko, R. Savkina, M. Smoliy, R. Udovyt'ska, F. Sizov, *Ukr. J. Phys.* **58**, 872 (2013).
- [9] R.A. Lidin, L.L. Andreeva, V.A. Molochko, *Constants of Inorganic Substances*, Begell House, New York 1995.